Optimized Green-Naghdi equations for the modelling of waves nearshore transformations

Fabien Marche
UM2, I3M
Montpellier, France

Philippe Bonneton and Marion Tissier
U. Bordeaux 1, EPOC
Talence, France

David Lannes
ENS, DMA
Paris, France

Florent Chazel
UPS/INSA, IMT
Toulouse, France

ABSTRACT

The fully nonlinear and weakly dispersive Green-Naghdi equations for shallow water waves of large amplitude is studied. An hybrid finite volume and finite difference splitting approach is proposed. Numerical validations are then performed in one horizontal dimension.

INTRODUCTION

In the study of nearshore dynamics, the propagation and transformations of waves in shallow water play a key role. An accurate modelling of associated processes, such as wave-breaking and swash motions, is a paramount for the study of coastal flooding due to storm waves or tsunamis, or to improve the prediction of short-term beach evolution, since they are the main source of sediment transport in the nearshore.

Modelling these processes requires a phase-resolving model, able to accurately describe wave-breaking and run-up over strongly varying topographies. In an incompressible and homogeneous fluid, the propagation of surface waves is described in its full generality by the Navier-Stokes equations with nonlinear boundary conditions at the surface and at the bottom. But this problem is highly computationally demanding, and therefore is not suitable for large scale propagation applications. Therefore, more simple models have been derived to describe the behavior of the solution in some physical specific regimes. They are based on Nonlinear Shallow Water (NSW) or Boussinesq-type (BT) equations. The reader is referred to (Lannes and Bonneton, 2009) for a study of the various shallow-water regimes.

Both nonlinear and dispersive effects can be accounted for by BT equations, with various degrees of accuracy. As the wave dynamic becomes strongly nonlinear in the final stages of shoaling and in the surf and swash zones, fully nonlinear equations, such as the Green-Naghdi (GN) equations are required (Green and Naghdi, 1976).

The GN equations provide a correct description of the waves up to the breaking point. But these equations do not intrinsically include energy dissipation due to wave breaking. Several attempts have been made to introduce wave breaking in Boussinesq-like models with the addition of ad hoc viscous terms to the equations, whose role is to account for the energy dissipation that occurs during wave breaking, see (Kennedy et al, 1999; Chen et al, 2000 and Cienfuegos et al, 2009) for instance.
Another approach to handle wave breaking is to use the NSW equations. These equations give an accurate description of the dissipation of energy during wave breaking. Broken waves are regarded as shocks and shock-capturing techniques, embedded in robust numerical solvers, allow for an accurate representation of broken wave dissipation and swash oscillations without any parameterization (Bonneton, 2007; Marche et al. 2007). However, this approach is inappropriate in the shoaling zone since this models neglects the nonhydrostatic and dispersive effects. The motivation of the work developped in (Bonneton et al, 2011) is to develop a model and a numerical scheme that describes correctly both phenomena: dispersive effects (in the shoaling zone in particular), wave breaking (in a simple way) and possibility of vanishing depth and dispersive effects, at the same time.

In this paper, we first briefly recall the new physical model introduced in (Bonneton et al, 2010), more suitable for numerical computations than the original GN equations. The next section is devoted to a brief presentation of the numerical scheme and of the new wave-breaking process embedded in our numerical model. Finally, we present several numerical validations. The propagation and nonlinear shoaling of solitary waves over regular sloping beaches is investigated. Run-up and run-down of a breaking solitary wave are also studied. A validation of our new simple numerical breaking process is highlighted (Tissier et al, 2010) and the last test case is devoted to the generation and propagation of undular bores (Tissier et al, 2011).

THE PHYSICAL MODEL

Throughout this paper, we denote by $\zeta(t, X)$ the elevation of the surface with respect to its rest state, and by $-h_0 + b(X)$ a parametrization of the bottom, where h_0 is a reference depth. Here X stands for the horizontal variables ($X = (x, y)$ for $2D$ surface waves, and $X = x$ for $1D$ surface waves), and t is the

time variable; we also denote by z the vertical variable.
where $h = h_0 + \zeta - b$ is the water depth. We thus have $V = (u, v) \in \mathbb{R}^2$ for $2D$ surface waves, and $V = u \in \mathbb{R}$ for $1D$ surface waves.
It is shown in (Bonneton et al, 2010) and (Chazel et al, 2011) that the usual GN equations are asymptotically equivalent to the following system :

$$\begin{cases} \partial_t h + \nabla \cdot (hV) = 0, \\ \partial_t (hV) + \nabla \cdot (hV \otimes V) + (I + h\mathcal{T}\frac{1}{h})^{-1}[gh\nabla\zeta + h\mathcal{Q}_1(V)] = 0, \end{cases} \tag{1}$$

where the operators $\mathcal{T}$ and $\mathcal{Q}_1$ are defined as follows :

$$\mathcal{T}[h,b]W = \mathcal{R}_1[h,b](\nabla \cdot W) + \mathcal{R}_2[h,b](\nabla b \cdot W) \tag{2}$$

$$\mathcal{Q}_1[h,b](V) = -2\mathcal{R}_1(\partial_1 V \cdot \partial_2 V^{\perp} + (\nabla \cdot V)^2) + \mathcal{R}_2(V \cdot (V \cdot \nabla)\nabla b) \tag{3}$$

$$\mathcal{R}_1[h,b]w = -\frac{1}{3h}\nabla(h^3 w) - \frac{h}{2}w\nabla b, \tag{4}$$

$$\mathcal{R}_2[h,b]w = \frac{1}{2h}\nabla(h^2 w) + w\nabla b. \tag{5}$$

It is worth mentionning that this new formulation does not involve any third order derivatives: this is a suitable property for the mathematical and numerical analysis.

Looking at the linearization of (1) around the rest state $h = h_0$, $V = 0$, and flat bottom $b = 0$, one derives the dispersion relation associated to (1). It is found by looking for plane wave solutions of the form $(\underline{h}, \underline{hV})e^{i(\mathbf{k}\cdot x - \omega t)}$ to the linearized equations, and consists of two branches parametrized by $\omega_{\alpha,\pm}(\cdot)$,

$$\omega_{\alpha,\pm}(\mathbf{k}) = \pm|\mathbf{k}|\sqrt{gh_0}\sqrt{\frac{1}{1 + (|\mathbf{k}|h_0)^2/3}}. \tag{6}$$

NUMERICAL METHOD

This new formulation is well-suited for a splitting approach separating the hyperbolic and the dispersive part of the equations (1). We use here a second order splitting scheme, where $S_1(\cdot)$ is the solution operator associated to the NSW equations and $S_2(\cdot)$ the solution operator associated to the dispersive part of the equations.

The splitting scheme

We compute the approximation $U^{n+1} = (\zeta^{n+1}, V^{n+1})$ at time $(n+1)\delta_t$ in terms of the approximation U^n at time $n\delta_t$ by solving

$$U^{n+1} = S_1(\delta_t/2)S_2(\delta_t)S_1(\delta_t/2)U^n,$$

with $S_1(t)$ the solution operator associated to NSWE:

$$\begin{cases} \partial_t h + \nabla \cdot (hV) = 0, \\ \partial_t (hV) + \nabla(\frac{1}{2}gh^2) + \nabla \cdot (hV \otimes V) = -gh\nabla b, \end{cases} \tag{7}$$

and $S_2(t)$ the solution operator associated to the dispersive part of the equations,

$$\begin{cases} \partial_t h = 0, \\ \partial_t (hV) - \frac{1}{\alpha}gh\nabla\zeta + (I + \alpha h\mathcal{T}\frac{1}{h})^{-1}[\frac{1}{\alpha}gh\nabla\zeta + h\mathcal{Q}_1(V)] = 0. \end{cases} \tag{8}$$

From this point, *we only consider* $1D$ *surface waves.*
For the numerical computation of $S_1(\cdot)$, we use a high order, robust and well-balanced finite volume method, based on a relaxation approach (Berthon and Marche, 2008). This method is known to be computationally cheap and very efficient to handle wave breaking and presents another interesting feature for our purposes: it allows the localisation of the shocks. To achieve a second order accuracy, we use the modified ENO scheme detailed in (Bouchut, 2004) for instance. The robustness of the resulting second order scheme is shown in (Berthon and Marche, 2008). We finally introduce a well-balanced discretization of the topography source term, using the hydrostatic reconstruction introduced in (Bouchut, 2004).

In the vicinity of the shocks (or bores to use the physical term) the derivation of the dispersive components of the GN equation is meaningless. We therefore "skip" the computation of $S_2(\cdot)$ near the shocks detected during the computation of $S_1(\delta_t/2)$. Elsewhere, $S_2(\cdot)$ is computed using a finite difference scheme (note that a careful mathematical analysis of $S_2(\cdot)$ allows considerable simplifications and numerical improvements).

As far as time discretization is concerned, we choose to use explicit methods. The systems corresponding to S_1 and S_2 are integrated in time using a classical fourth-order Runge-Kutta scheme. Details concerning the numerical method can be found in (Bonneton et al, 2010).

WAVE BREAKING

To handle wave breaking, we switch to NSW equations locally in space and time, by skipping the dispersive step S_2 when the wave is ready to break. The coupling between the two sets of equations is thus performed in a natural way, without implementing any boundary conditions. As we aim at applying our code to realistic incoming waves, implying different locations of the breaking point, we need to handle each wave individually. We present in this section a simple way to detect wave fronts at each time step, as well as the criterion to initiate and terminate breaking.

Detection of the wave fronts

To decide where to suppress the dispersive step, we use the first step S_1 of the time-splitting as a predictor to assess the local energy dissipation. It can be expressed as:

$$D_i(x,t) = -\left(\frac{\partial E}{\partial t} + \frac{\partial F}{\partial t}\right), \tag{9}$$

with

$$E = \frac{\rho}{2}\left(hu^2 + g((h+b)^2 - b^2)\right), \quad F = \rho hu\left(\frac{u^2}{2} + g(h+b)\right), \tag{10}$$

the energy and the energy flux densities. The local dissipation is close to zero in regular wave regions and forms peaks when shocks are appearing. We can then locate the future breaking wave fronts at each time step, and eventually skip the following step S_2 in their vicinities (Tissier et al. 2010).

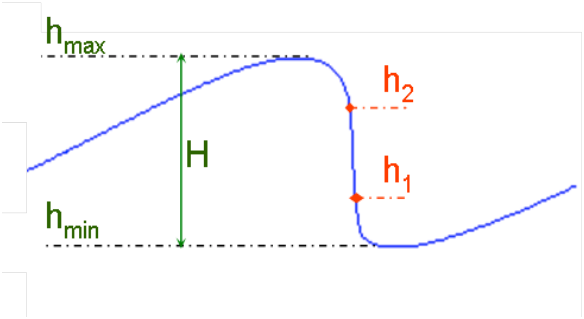

Figure 1: Definition sketch.

Characterization of breaking

To characterize each wave front individually, the local dissipation is integrated over the front and normalized by the theoretical dissipation, given by the shock theory:

$$D_{th} = \frac{\rho g}{4}\left(\frac{g(h_1+h_2)}{2h_1h_2}\right)^{\frac{1}{2}}(h_2-h_1)^3, \tag{11}$$

where D_{th} is the energy dissipated across the shock, with h_1 and h_2 the water heights in front and behind the shock (see Figure 1). From a practical point of view, h_1 and h_2 are approximated by the local minimum and maximum of h which are the closest to the peak of dissipation, and therefore D_{th} is estimated by:

$$D_{th} \approx \frac{\rho g}{4}\left(\frac{g(h_{min}+h_{max})}{2h_{min}h_{max}}\right)^{\frac{1}{2}}H^3. \tag{12}$$

A mixed breaking criterion

The study of the energy dissipation needs to be combined with a criterion for the initiation of breaking. We use here a criterion based on the front slope, initially introduced in (Schaffer et al, 1993). Two angles are then defined. Φ_i corresponds to the angle at which the breaking process starts, and Φ_f, the angle at which the breaking process stops. We choose $\Phi_i = 30\,^\circ$ and $\Phi_f = 8\,^\circ$, which are the optimal angles determined in (Cienfuegos et al, 2010) for their Serre model. Finally, the following method is applied in order to handle wave breaking at each time step. Potentially breaking wave fronts are first located thanks to the energy dissipation. For each of them, we compute the value of the front slope and the normalized dissipation. Finally, we decide if we switch locally from one set of equations to the other depending on the values of these two parameters.

As several wave fronts can be detected at each time step, either breaking or not, the width of the zone (centred on the peak of dissipation) where the switch to NSWE is performed needs to be defined. It must be of the order of magnitude of the physical length of the roller, which is roughly proportional to the wave height. A detailed study of the breaking mechanism is performed in (Tissier et al, 2010; Tissier et al, 2011).

NUMERICAL VALIDATIONS

In this section we focus on some test cases. The first one is devoted to assess that the balance between non-linear and dispersive effects is preserved by our splitting approach. In the second test, we show that the use of a finite-volume scheme for the hyperbolic part of the equations leads to an accurate description of the shoreline motions.

Incident wave amplitude: $a_0/h_0 = 0.096$					
Gauge location (m) (relative to the shoreline)	2.430	2.215	1.960	1.740	1.502
Relative amplitude error (%)	-1.6	-2.5	-5.5	-7.1	-10.9
Incident wave amplitude: $a_0/h_0 = 0.298$					
Gauge location (m) (relative to the shoreline)	3.980	3.765	3.510	3.290	3.052
Relative amplitude error (%)	1.2	-0.5	0.2	-0.2	0.04
Incident wave amplitude: $a_0/h_0 = 0.456$					
Gauge location (m) (relative to the shoreline)	4.910	4.695	4.440	4.220	3.982
Relative amplitude error (%)	3.6	-0.3	1.1	0.5	2.2
Incident wave amplitude: $a_0/h_0 = 0.534$					
Gauge location (m) (relative to the shoreline)	5.180	4.965	4.710	4.490	4.252
Relative amplitude error (%)	0.03	-0.1	-1.4	-1.7	0.7

Table 1: Location of wave gauges for solitary waves shoaling on a 1:30 sloped beach, and relative error between the computed and measured wave amplitudes at each gauge.

Nonlinear shoaling of solitary waves propagating over a beach

We investigate in this test the ability of the scheme to simulate the nonlinear shoaling of solitary waves over regular sloping beaches, which is a paramount in the study of nearshore propagating waves. This test is based on the experiments performed at the LEGI, in Grenoble (France) and reported in (Guibourg, 1994). Solitary waves are generated in a $36\,m$ long wave-flume.

Free surface displacements were measured at various locations, using wave gauges located just before breaking. Four solitary waves of different heights are generated (see Table 1), in order to account for various nonlinearity effects during propagation towards the shore.

All simulations are performed using $\delta_x = 0.025\,m$ and $\delta_t = 0.016\,s$. The initial water depth is $h_0 = 0.25\,m$ in the horizontal part of the channel.

Results are shown for each configuration in terms of time-series at the wave gauges locations in Figure 2. The relative error between computed and measured wave amplitudes is presented in Table 1. The global agreement is good, both for the amplitude and shape of the solitary waves. Significant errors can be observed for the less nonlinear case ($a_0/h_0 = 0.096$), but the discrepancies can be partly explained by experimental problems, since it can be observed that the water surface is not totally at rest before the propagation of the solitary wave. Note that validations based on

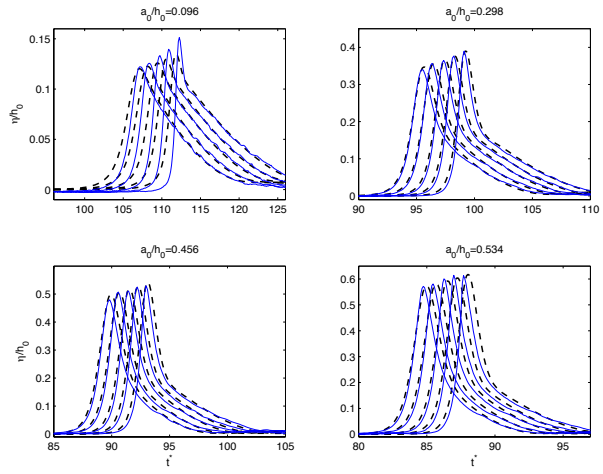

Figure 2: Nonlinear shoaling of solitary waves propagating over a beach - Time series of the free surface elevation for the solitary wave propagating over the 1:30 sloping beach. (—) experimental data, (- - -) numerical results, with $t^* = t(g/h_0)^{1/2}$.

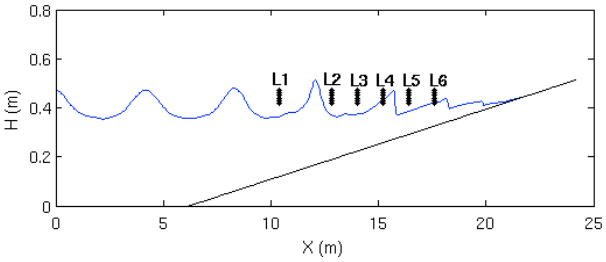

Figure 3: Definition sketch for Cox experiment (1995). Vertical lines (L1 to L6) correspond to the locations of the wave gauges. The free surface has been computed using the S-GN model.

more demanding test cases, with strongly dispersive waves, have been done in (Chazel et al, 2011).

Cox experiment

We consider in this test Cox's regular waves experiment (Cox, 1995). Cnoidal waves of relative amplitude $H/h_0 = 0.29$ and period $T = 2.2\,s$ were generated in the horizontal part of a wave flume, of depth $h_0 = 0.4\,m$. They were then propagating and breaking on a 1:35 plane beach. For this test case, synchronized time-series of free surface elevation are available at six locations, corresponding to wave gages located outside (L1 and L2) and inside (L3 to L6) the surf zone (see Figure 3). The experimental breaking point is located slightly shoreward to L2.
Figure 4 compares the experimental and numerical time-series for this experiment. It is worth noting that the time-series are in phase, demonstrating that wave celerity is accurately predicted by the model. We have a very good overall agreement concerning the shape of the waves, both in the shoaling and surf zone. In particular, the model is able to reproduce the typical saw-tooth profile in the inner surf zone.

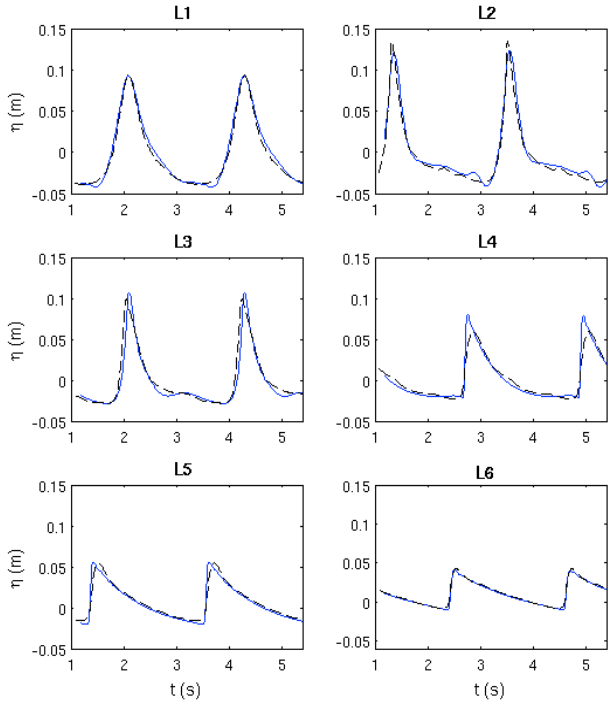

Figure 4: Comparisons of computed (blue lines) and experimental synchronized time-series of free-surface elevation at the wave gauges for Cox breaking experiment (1995).

Run-up and run-down of a breaking solitary wave over a planar beach

This test is based on experiments carried out in (Synolakis, 1987) for an incident solitary wave of relative amplitude $a_0/h_0 = 0.28$, which propagates and breaks over a planar beach with a slope of 1:19.85. Free surface elevations at different times are available thanks to video measurements.

The still water level in the horizontal part of the beach is $h_0 = 0.3\,m$. The simulations are performed using the cell size $\delta_x = 0.08\,m$ and $\delta_t = 0.02\,s$.

The comparison between measured and computed waves is presented in Figure 5. It shows a good agreement between model predictions and laboratory data and illustrates the ability of our model to reproduce shoaling, breaking, run-up and run-down, as well as the formation and breaking of the backwash bore.

Undular bores propagation

Tsunamis propagating in the open ocean are basically non dispersive long waves. However, the integration of weak dispersive effects can become significant when the propagation takes place over a long time, and end up modifying the tsunami waves. Dispersive effects finally become significant in shallow-water regions (Grue et al., 2008). In the nearshore, the competition between non-linearities, dispersive effects and energy dissipation will govern the transformation of tsunami wave fronts. They can evolve into a large range of bore types, from undular non-breaking bore to purely breaking bore. In this test case, we investigate the ability of our numerical model to predict bore dynamics. The

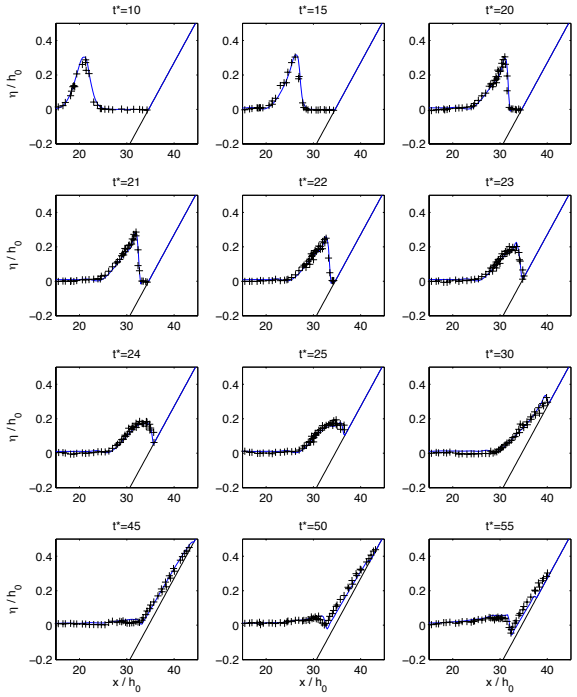

Figure 5: Comparisons of model predictions (—) and experimental snapshots (+) for a breaking solitary wave, on a 1 : 19.85 constant slope beach, with $t^* = t(g/h_0)^{1/2}$.

model is applied to the formation of undular bores, and compared with laboratory data obtained in (Soares-Frazao and Zech, 2002). We consider a channel initially at rest with an initial water height $h_0 = 0.251\,m$. At $t = 0s$, we impose a discharge at the gate $Q_0 = 0.06\,m^3.s^{-1}$. The Froude number of the resulting bore is Fr=1.104. For the simulations, the grid size of the mesh is $\delta x = 0.2\,m$ and we consider a Courant number of 0.9. Figure 6 compares experimental and numerical time-series of water elevation at the wave gauges. It shows that the model predicts accurately the bore celerity, and that the agreement is good in term of amplitude and wavelength of the secondary waves. It can be noticed that the growth of the first wave is faster in the experiments than predicted by our numerical model. The ability of our model to predict the different bore shapes is investigated in (Tissier et al, 2011), together with the effects of the bore transformation on wave run-up over a sloping beach.

CONCLUSION

We have developed a numerical for a new GN set of equations, particularly suitable for numerical discretization. Extended numerical validations are proposed. First academic and analytic cases (solitary waves propagation) are shown. We clearly demonstrate the robustness and the ability of our model to take into account wave propagations over varying topography, including wave shoaling, wave breaking, run-up and generation of undular bores.

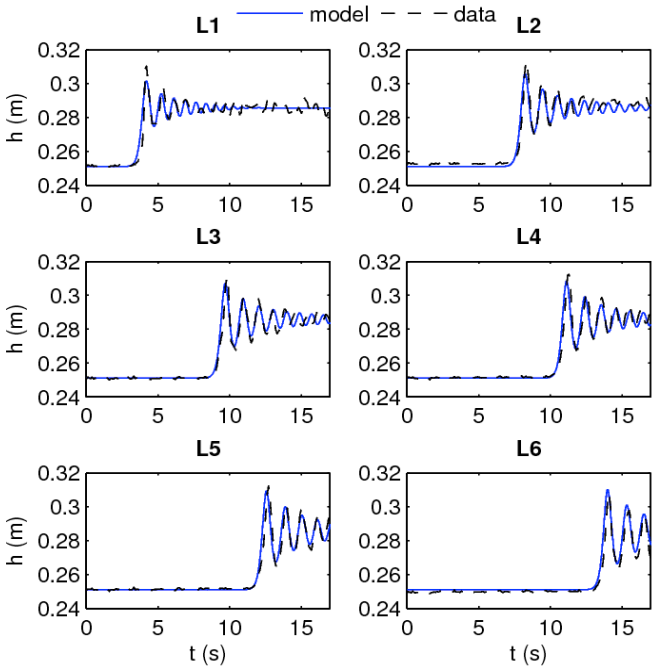

Figure 6: Water level evolution as a function of time at 6 gauges. Comparisons between experimental data (dashed lines) from (Soares-Frazao and Zech, 2002) and model prediction (plain lines). Fr=1.104.

REFERENCES

Berthon, C and Marche, F (2008). "A Positive Preserving High Order VFRoe Scheme for Shallow Water Equations: A Class of Relaxation Schemes", *SIAM J. Sci. Comput.*, Vol 30(5), pp 2587–2612.

Bonneton, P (2007). "Modelling of periodic wave transformation in the inner surf zone", *Ocean Engineering*, Vol 34, pp 1459–1471.

Bonneton, P, Chazel, F, Lannes, D, Marche, F and Tissier, M (2010a). "A splitting approach for the fully nonlinear and weakly dispersive Green-Naghdi model", *J.Comput. Phys.*, Vol 230(4), pp 1479-1498.

Bouchut, F (2004). "Nonlinear stability of Finite Volume Methods for Hyperbolic Conservation Laws and Well-Balanced Schemes for Sources", Frontiers in Mathematics, Birkhauser.

Brocchini, M and Dodd, N (2008). "Nonlinear shallow water equation modeling for coastal engineering", *J. Wtrwy. Port, Coast. and Oc. Engrg*, Vol 134(2), pp 104–120.

P, Chazel, F, Lannes, D, Marche, F (2011). "Numerical simulation of strongly nonlinear and dispersive waves using a Green-Naghdi model", to appear in *J. Sci. Comput.*, DOI: 10.1007/s10915-010-9395-9.

Chen, Q, Kirby, JT, Dalrymple, RA, Kennedy, AB and Chawla, A (2000). "Boussinesq modeling of wave transformation, breaking, and runup. II: 2d", *J. Wtrwy., Port, Coast., and Oc. Engrg.*, Vol 126, pp 48–56.

Cienfuegos, R, Barthelemy, E and Bonneton, P (2007). "A fourth-order compact finite volume scheme for fully nonlinear and weakly

dispersive Boussinesq-type equations. Part II: Boundary conditions and validations", *Int. J. Numer. Meth. Fluids*, Vol 53, pp 1423–1455.

Cienfuegos, R, Barthelemy, E and Bonneton, P (2010). "A wave-breaking model for Boussinesq-type equations including mass-induced effects", *J. Wtrwy., Port, Coast., and Oc. Engrg.*, Vol 136, pp 10–26.

Cox, D (1995). "Experimental and numerical modelling of surf zone hydrodynamics". PhD thesis, University of Delaware, Newark, Del.

Godlewski, E and Raviart, PA (1996). "Numerical approximation of hyperbolic systems of conservation laws", Applied Mathematical Sciences 118, Springer.

Green, AE and Naghdi, PM (1976). "A derivation of equations for wave propagation in water of variable depth", *Journal of Fluid Mechanics*, Vol 78(2), pp 237–246.

Guibourg, S (1994). "Modélisation numérique et expérimentale des houles bidimensionnelles en zone cotière", PhD Thesis, Université Joseph Fourier - Grenoble I, France.

Grue, J, Pelinovsky, EN, Fructus, D, Talipova, T and Kharif, C (2008). "Formation of undular bores and solitary waves in the Strait of Malacca caused by the 26 December 2004 Indian Ocean tsunami". *Journal of Geophysical Research*, Vol 113.

Kennedy, AB, Chen, Q, Kirby, JT and Dalrymple, RA (1999). "Boussinesq modeling of wave transformation, breaking, and runup. I: 1D", *J. Wtrwy., Port, Coast., and Oc. Engrg.*, Vol 126, pp 39–47.

Lannes, D and Bonneton, P (2009). "Derivation of asymptotic two-dimensional time-dependent equations for surface water wave propagation", *Physics of Fluids*, Vol 21(1).

Marche, F, Bonneton, P, Fabrie, P and Seguin, N (2007). "Evaluation of well-balanced bore-capturing schemes for 2D wetting and drying processes", *Internat. J. Numer. Methods Fluids*, Vol 53(5), pp 867–894.

Peregrine, DH (1967). "Long waves on a beach", *Journal of Fluid Mechanics*, Vol 27, pp 815–827.

Serre, F (1953). "Contribution à lâĂŹ étude des écoulements permanents et variables dans les canaux", *Houille Blanche*, Vol 8, pp 374 âĂŞ388.

Schaffer, H.A., Madsen, PA and Deigaard, R (1993). "A Boussinesq model for waves breaking in shallow water", *Coastal Engineering*, Vol 20, pp 185-202.

Soares-Frazao S and Zech Y (2002). "Undular bores and secondary waves. Experiments and hybrid finite-volume modeling", *Journal of Hydraulic Research*, Vol 40 (1), pp 33-43.

Synolakis, CE (1987). "The runup of solitary waves", *Journal of Fluid Mechanics*, Vol 185, pp 523–545.

Tissier, M, Bonneton, P, Chazel, F, Lannes, D and Marche, F (2010) "Serre Green-Naghdi modelling of wave transformation breaking and run-up using a high-order finite-volume finite-difference scheme", *Proceedings of International Conference in Coastal Engineering, 2010.*

Tissier, M, Bonneton, P, Marche, F, Chazel, F and Lannes, D (2011). "Nearshore Dynamics of Tsunami-like Undular Bores using a Fully Nonlinear Boussinesq Model ", to appear in *Journal of Coastal Research.*

Wei, G and Kirby, JT (1995). "A time-dependent numerical code for extended Boussinesq equations", *J. Wtrwy., Port, Coast., and Oc. Engrg.*, Vol 120, pp 251–261.